Additive Covalent Radii for Single-, Double-, and Triple-Bonded Molecules and Tetrahedrally Bonded Crystals: A Summary

ARTICLE *in* THE JOURNAL OF PHYSICAL CHEMISTRY A · AUGUST 2014

Impact Factor: 2.69 · DOI: 10.1021/jp5065819 · Source: PubMed

1 AUTHOR:

Pekka Pyykkö
University of Helsinki

325 PUBLICATIONS **14,349** CITATIONS

SEE PROFILE

THE JOURNAL OF PHYSICAL CHEMISTRY A

Article

pubs.acs.org/JPCA

Additive Covalent Radii for Single-, Double-, and Triple-Bonded Molecules and Tetrahedrally Bonded Crystals: A Summary

Pekka Pyykkö*

Department of Chemistry, University of Helsinki, POB 55 (A. I. Virtasen aukio 1), 00014 Helsinki, Finland

ABSTRACT: The recent fits of additive covalent radii $R_{AB} = r_A + r_B$ for the title systems are reviewed and compared with alternative systems of radii by other authors or with further experimental data. The agreement of the predicted R with experiment is good, provided that the A−B bond is not too ionic, or the coordination numbers of the two atoms too different from the original input data, used in the fit. Bonds between transition metals and halides are not included in the single-bond set, because of their partial multiple-bond character.

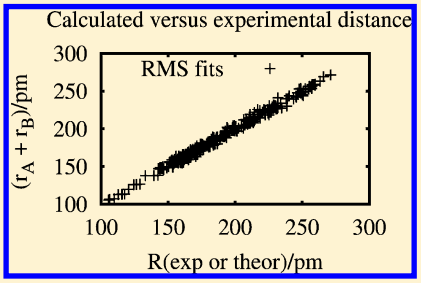

1. INTRODUCTION

The purpose of additive covalent radii is to approximate a bond length as the sum of two atomic radii,

$$R_{AB} = r_A + r_B \quad (1)$$

We have recently presented new sets of such covalent radii for single,[1] double,[2] and triple bonds,[3] primarily for molecules that are predominantly covalent. A set for tetrahedrally bonded crystals was also published.[4] The mean-square deviations of these fits were about 3 pm in the three molecular cases and 0.7 pm for the crystals. We consider these radii as purely operational; i.e., we do not try to derive them from fundamental theories. In our fits, both experimental, and theoretical ab initio data are used for R. No data were interpolated nor guessed.

A single bond is here defined as one, having a predominant σ^2 bonding orbital as in ethane, H_3C-CH_3, or having a corresponding net excess of bonding minus antibonding orbitals, as in Cl_2. A double bond has similarly $\sigma^2\pi^2$ bonding orbitals, and a triple bond, $\sigma^2\pi^4$ bonding orbitals. These are taken as the definition of single-, double-, or triple-bond character. It does not matter if an ab initio calculation gives some different, fractional bond order. Strongly ionic systems remain outside the present discussion.

A crucial observation was to note that TM−X bonds between transition metals, TM, and halogens, X, had to be omitted from the single-bond data set, because they have a partial multiple-bond character, due to some π back-donation from X to TM.[1] Certain other outliers also had to be omitted in each data set. These are discussed in the original papers. Similarly, the typical coordination numbers, CN, and oxidation states of the molecular input data are described there.

A notable predecessor of such fits was Pauling.[5] Others exist and were quoted in the references cited earlier. Slater[6] derived additive, general-purpose atomic radii which cover covalent, ionic, and metallic molecules and solids for elements 1−95 with an average error of 12 pm. Another recent fit for single bonds, using the Cambridge Structural Data Base, is that of Cordero et al.[7] The differences in philosophy are discussed in Table 1 and arise from the data source, the sample size, the elements considered, and self-consistency versus fixing certain radii. The latter means setting certain radii, as done by Pauling, equal to half their homonuclear bond length:

$$r_E = R_{E-E}/2 \quad (2)$$

or to introducing different single-bond radii for sp^3-, sp^2-, and sp-hybridized carbons.[7] Mantina et al.[8] simply took the average of the two covalent radii of Cordero et al. and Pyykkö et al.

A parallel problem is that of determining ionic radii for crystals. It goes back to Bragg[9] or Wasastjerna.[10] A widely used fit is the one by Shannon and Prewitt[11] or Shannon.[12] Their "IR" set is based on fixing $r(O^{2-}, CN=6)$ and $r(F^-, CN=6)$ at 140 and 133 pm, respectively. Similarly, the "CR" set has 126 and 119 pm for oxide and fluoride, respectively. For recent summaries, see Gibbs et al.[13] or Liu et al.[14]

A further option, not discussed here, is to go beyond these simply additive "hard-sphere radii" and to introduce "soft-sphere

Table 1. Differences in Methods for Determining Single-Bond Covalent Radii in Reference 1 and Reference 7[a]

property	ref 1	ref 7
data source	expt or calc	expt (CSD)
sample size	410 points	172000
elements	1−118	1−96
self-consistency	yes	no

[a]CSD stands for the Cambridge Structural Data Base.

Special Issue: Markku Räsänen Festschrift

Received: July 2, 2014
Revised: August 27, 2014
Published: August 27, 2014

   dx.doi.org/10.1021/jp5065819 | J. Phys. Chem. A 2015, 119, 2326−2337

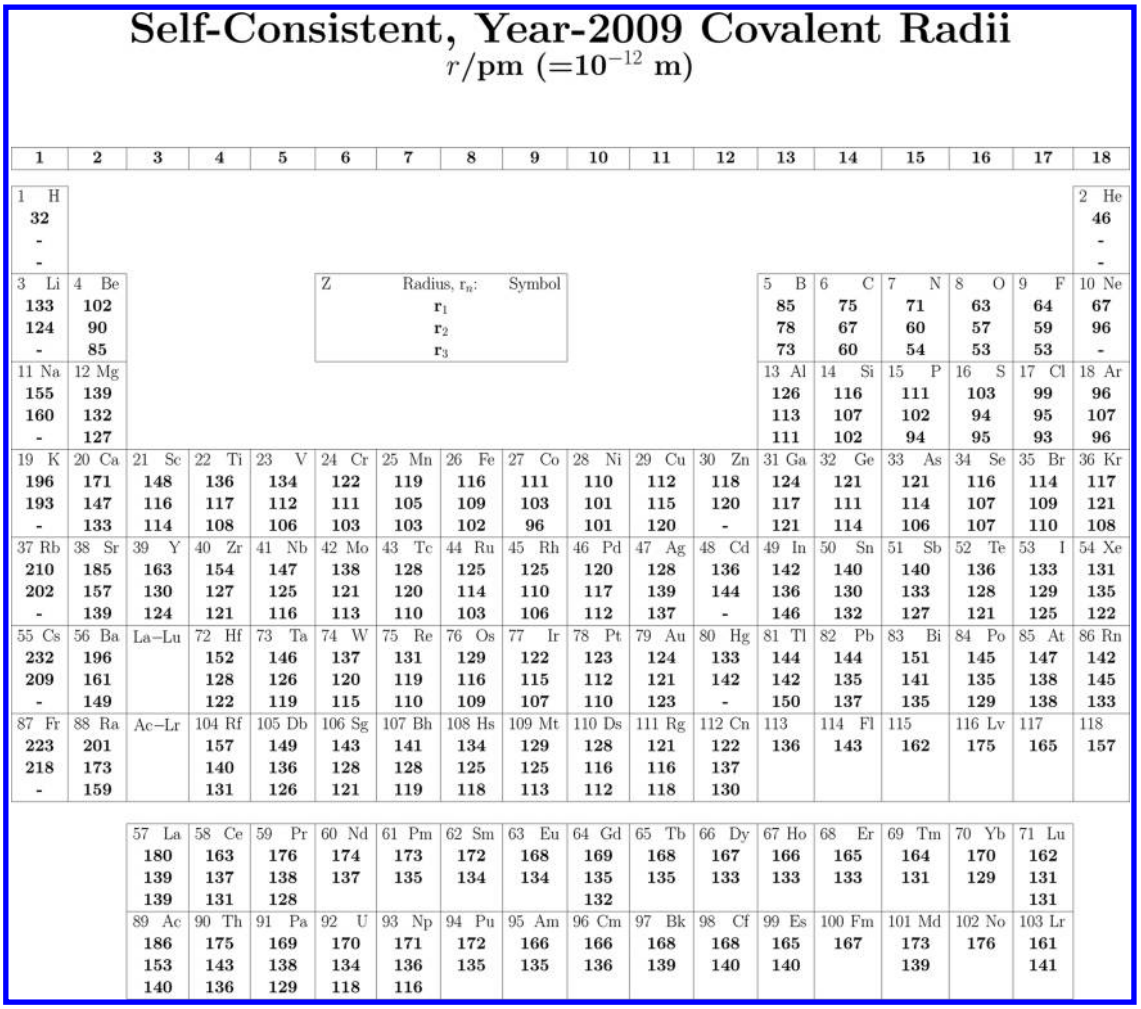

1	2	3	4	5	6	7	8	9	10	11	12	13	14	15	16	17	18
1 H 32 - -																	2 He 46 - -
3 Li 133 124 -	4 Be 102 90 85											5 B 85 78 73	6 C 75 67 60	7 N 71 60 54	8 O 63 57 53	9 F 64 59 53	10 Ne 67 96 -
11 Na 155 160 -	12 Mg 139 132 127											13 Al 126 113 111	14 Si 116 107 102	15 P 111 102 94	16 S 103 94 95	17 Cl 99 95 93	18 Ar 96 107 96
19 K 196 193 -	20 Ca 171 147 133	21 Sc 148 116 114	22 Ti 136 117 108	23 V 134 112 106	24 Cr 122 111 103	25 Mn 119 105 103	26 Fe 116 109 102	27 Co 111 103 96	28 Ni 110 101 101	29 Cu 112 115 120	30 Zn 118 120 -	31 Ga 124 117 121	32 Ge 121 111 114	33 As 121 114 106	34 Se 116 107 107	35 Br 114 109 110	36 Kr 117 121 108
37 Rb 210 202 -	38 Sr 185 157 139	39 Y 163 130 124	40 Zr 154 127 121	41 Nb 147 125 116	42 Mo 138 121 113	43 Tc 128 120 110	44 Ru 125 114 103	45 Rh 125 110 106	46 Pd 120 117 112	47 Ag 128 139 137	48 Cd 136 144 -	49 In 142 136 146	50 Sn 140 130 132	51 Sb 140 133 127	52 Te 136 128 121	53 I 133 129 125	54 Xe 131 135 122
55 Cs 232 209 -	56 Ba 196 161 149	La–Lu	72 Hf 152 128 122	73 Ta 146 126 119	74 W 137 120 115	75 Re 131 119 110	76 Os 129 116 109	77 Ir 122 115 107	78 Pt 123 112 110	79 Au 124 121 123	80 Hg 133 142 -	81 Tl 144 142 150	82 Pb 144 135 137	83 Bi 151 141 135	84 Po 145 135 129	85 At 147 138 138	86 Rn 142 145 133
87 Fr 223 218 -	88 Ra 201 173 159	Ac–Lr	104 Rf 157 140 131	105 Db 149 136 126	106 Sg 143 128 121	107 Bh 141 128 119	108 Hs 134 125 118	109 Mt 129 125 113	110 Ds 128 116 112	111 Rg 121 116 118	112 Cn 122 137 130	113 136	114 Fl 143	115 162	116 Lv 175	117 165	118 157

57 La	58 Ce	59 Pr	60 Nd	61 Pm	62 Sm	63 Eu	64 Gd	65 Tb	66 Dy	67 Ho	68 Er	69 Tm	70 Yb	71 Lu
180 139 139	163 137 131	176 138 128	174 137	173 135	172 134	168 134	169 135 132	168 135	167 133	166 133	165 133	164 131	170 129	162 131 131
89 Ac	90 Th	91 Pa	92 U	93 Np	94 Pu	95 Am	96 Cm	97 Bk	98 Cf	99 Es	100 Fm	101 Md	102 No	103 Lr
186 153 140	175 143 136	169 138 129	170 134 118	171 136 116	172 135	166 135	166 136	168 139	168 140	165 140	167	173 139	176	161 141

Figure 1. Present single-, double-, and triple-bond radii for molecules (r_1, r_2, and r_3), respectively, in picometers (pm). Adapted with permission from ref 2. Copyright 2009 Wiley-VCH.

radii" with further parameters, see Lang and Smith,[15] or to make a Schomaker–Stevenson[16] electronegativity correction.[17] With more parameters per element, improved fits could be hoped for. Their procedure can also be applied to strongly ionic molecules, such as the diatomic alkali halides, outside the applicability of the present, additive hard-sphere radii. In that sense they bridge covalent and ionic bonding. Criticism concerning the Schomaker–Stevenson equation has also been raised.[18]

2. PRESENT RADII AND COMPARISONS WITH OTHER SETS

All present radii for molecules are shown in Figure 1 and those for tetrahedral crystals in Figure 2. The single-bond radii are given and compared with a number of predecessors in Table 2. A similar comparison is made for the double-bond and triple-bond cases in Tables 3 and 4, respectively.

3. COMPARISONS WITH LATER EXPERIMENTAL DATA

3.1. "Narrow Fit" for Diatomic Interalkalis. In ref 1 we also made a special fit to the R_e of the MM′ interalkali diatomics. The standard deviation δ was only 0.84 pm. The resulting radii, r_1, were 134.3, 153.9, 195.9, 210.4, and 232.2 pm for Li–Cs, respectively. At the time, the experimental R_e were still unknown for diatomic LiRb and KCs. These radii would predict 344.7 and 428.1 pm, respectively. Later experiments give an R_e = 346.6[20] and 428.4 pm,[21] for LiRb and KCs, respectively, in adequate agreement. We repeat here that the r_1(Cs) of "253 pm", given in certain sources, seems to be a perpetuated misprint of an earlier value of 235 pm,[22] close to the present values.

3.2. Some General Comparisons and Anomalies. *Boron Trihalides and Carbocations.* The present r_1(B) of 85 pm is based on BH_3 and BMe_3. Also BH_4^- would fit (R(B–H) of 117 pm (calc) and 119 pm (expt)[23] for terminal H in gaseous $Zr(BH_4)_4$ or up to 122 pm from neutron diffraction[24]). Although the trihalides BX_3 correspond to the usual halogen CN = 1, their experimental R(B–X) for X = Cl–I[25] would correspond to a clearly shorter r_1(B) of 75 pm. This can be attributed to X → B π back-donation, as in the isoelectronic carbocation CX_3^+ case.[26] Both of these are early p–late p combinations where one atom has available orbitals and the other atom has available electrons for multiple bonding. Note moreover the existence of the series BE_3^{3-}, E = S, Se. The typical experimental B–E distances are 183 and 195 pm for E = S and Se, respectively,[27] on the short side of the Σr_1.

B–N Bonds. The sums of the present radii are 156, 138, and 127 pm for single-, double-, and triple bonds, respectively. Berski et al.[28] report both experimental and computed values which for ammine boranes are on the long side, 163–170 pm. For double

dx.doi.org/10.1021/jp5065819 | J. Phys. Chem. A 2015, 119, 2326–2337

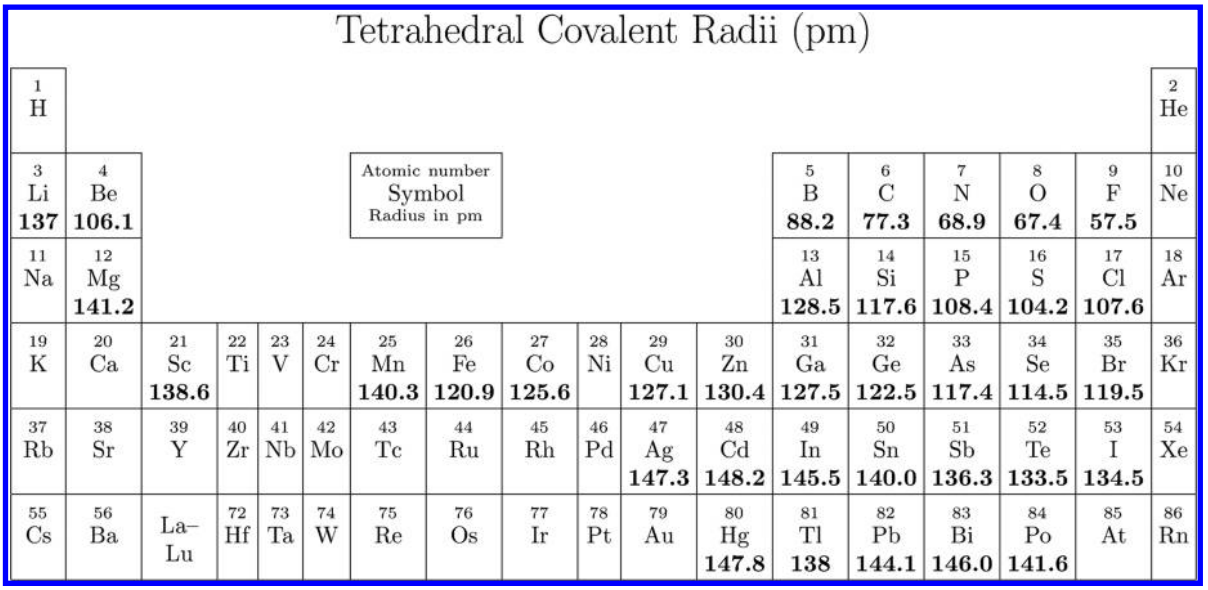

Figure 2. Covalent radii (pm) for tetrahedrally bonded crystals. Reprinted with permission from ref 4. Copyright 2012 American Physical Society.

and triple bonds their R are 138−139 and 123−126 pm, respectively. Berski et al. relate their bond orders to the electron localization function, ELF. Another review on B≡N bonds with similar results was published by Brand et al.[29]

Si−Cl Bonds Short. As discussed by Wells[18] in 1949, they are "short". The present Σr_1 is 215 pm, compared to typical experimental values[25] of 201−204 pm. The same comment can be made about P−Cl bonds. This is still a bit of a puzzle. Neither ionicity nor multiple bonding are obvious explanations.

Sulfate and Other Valence Isoelectronic Systems. The SO_4^{2-} group has typically an S−O bond length of about 149 pm,[25] comparable with the Σr_3 = 148 pm. A traditional way to discuss its bonding is in terms of various resonance structures; see Pauling.[5] These isoelectronic structures go all the way to the predicted ArO_4.[30−32]

Au−Au Bonds. A novel, unbridged 6s−6p_z−5d_{xy}-hybridized Au(II)−Au(II) bond of ≥250 pm was analyzed by Xiong and Pyykkö.[33] Because the three covalent radii r_1 to r_3 for Au are very close, it will not be possible to draw conclusions on the bond order based on the R(Au−Au) only. There were several experimental data for such compounds, but no previous theoretical analysis.

"Inverted Cases" $r_1 < r_2 < r_3$. In these cases the trend for the AB bond is simply weaker than the trend for the covalent radii of the individual atoms.

Effect of CN. In general, an increased n for AB_n will result in a larger R(AB). This will give a natural explanation to some differences between the radii of Cordero et al.[7] and the present r_1. The input data sets were simply different.

Hydrogen, H. The various molecular fits for r(H) give closely similar answers of 30−32 pm. If one used the homonuclear H_2 alone, 37 pm would be obtained. The possible reasons were discussed by Batsanov.[34] In the present fit that H_2 point was omitted as an outlier.

Fluorine, F. Considerable variation is found in the effective covalent radius of F; use ref 35 as a lead reference.

3.3. Single-Bond Radii. The present radii for covalent bonds in molecules have by now been quoted hundreds of times, mostly because they were found useful. See the ISI Web of Knowledge for examples. When comparing the present r_1 in Table 2 with those of Cordero et al.,[7] one finds that for the first 96 elements, 40 are within a few picometers (maximum 10 pm) from each other. The others are transition elements for which the coordination numbers are much larger for the crystallographic data used by Cordero, than for the molecular data, specified by Pyykkö and Atsumi.[1]

Some post-2009 cases in order of increasing (Z_1,Z_2) are as follows.

Boron−Boron Bonds. The structure of solid $LiB_{12}PC$ contains B−B bonds between the icosahedra with an average length of 172.7 pm.[36] Twice the single-bond radius is 170 pm. The same crystal structure has P−C distances of 186 pm, matching the present single-bond radii, 186 pm.

MX, M = Li−Cs and X = Cl−I. As said, these ionic diatomics lie outside the domain of applicability of the present radii. The radii of Lang and Smith[17] still work for these molecules. Note that all comparisons of our r_1 radii with the R values in Lang and Smith's "Table 14" are actually forbidden by either too strong ionicities or the mentioned exclusion of transition-metal−halide bonds, due to the partial multiple-bond character of the M−X bonds, as said in the Introduction.

MM′, M = Li−Cs. The present radii are excellent for the diatomic MM′,[1] as discussed in section 3.1.

Li−Bi. The bond length for both atoms bound near their respective porphyrins is 287.4 pm,[37] while the single-bond radii give 284 pm, thus supporting the idea of Li−Bi bonding in that molecule.

Be−Be. Although the dimer Be_2 is very weakly bound, the tetrahedral tetramer Be_4 has a calculated[38] Be−Be bond length of 203 pm (Σr_1 = 204 pm). The calculations of Ascik et al.[39] entirely agree, giving 204 pm.

Group 15. The experiments by Traut et al.[40] for P−Bi, As−Bi, As−As, and Te−Bi bonds give an R of 263, 271.7, 245, and 286 pm, compared to the sums of single-bond radii of 262, 272, 242, and 287 pm, respectively.

Pb−Se. The X-ray Pb−Se of the tetrahedral anion $[PbSe_4]^{4-}$ is 260−261 pm, compared with the sum of r_1 of 260 pm.[41]

Pb−Sm. Zeckert et al.[42] report in their molecule **2** an unbridged Pb−Sm bond of 326.6 pm. The present radii predicted 316 pm, while the Cordero et al.[7] radii give 344 pm,

dx.doi.org/10.1021/jp5065819 | J. Phys. Chem. A 2015, 119, 2326−2337

Table 2. Comparisons of Present Single-Bond Radii, r_1 ("PW", pm), with Some Earlier Values[a]

Z	E	PW	CN	Cordero[7]	Pauling[5]	Batsanov[19]	Z	E	PW	CN	Cordero[7]	Pauling[5]	Batsanov[19]
1	H	32	1	31	30	37	60	Nd	174	3	201		
2	He	46	1	28			61	Pm	173	3	199		
3	Li	133	1	128		134	62	Sm	172	3	198		
4	Be	102	2	96		98	63	Eu	168	3	198		
5	B	85	3	84	–	85	64	Gd	169	3	196		
6	C	75	4	76[b]	77.2	77	65	Tb	168	3	194		
7	N	71	3	71	70	73	66	Dy	167	3	192		
8	O	63	2	66	66	72	67	Ho	166	3	192		
9	F	64	1	57	64	71	68	Er	165	3	189		
10	Ne	67	1	58		–	69	Tm	164	3	190		
11	Na	155	1	166		165	70	Yb	170	3	187		
12	Mg	139	2	141		142	71	Lu	162	3	187		
13	Al	126	3	121		129	72	Hf	152	4	175		150
14	Si	116	4	111	117	118	73	Ta	146	4, 5	170		142
15	P	111	3	107	110	111	74	W	137	4, 6	162		136
16	S	103	2	105	104	103	75	Re	131	5	151		131
17	Cl	99	1	102	99	99	76	Os	129	4	144		129
18	Ar	96	1	106	–	–	77	Ir	122	3	141		135
19	K	196	1	203		200	78	Pt	123	2	136		130
20	Ca	171	2	176		173	79	Au	124	1	136		124
21	Sc	148	3	170		144	80	Hg	133	1, 2	132		133
22	Ti	136	4	160		135	81	Tl	144	3	145		148
23	V	134	4, 5	153		131	82	Pb	144	2, 4	146		147
24	Cr	122	6	139		132	83	Bi	151	3	148		150
25	Mn	119	5	150[c]		128	84	Po	145	2	140		143
26	Fe	116	4	142[c]		131	85	At	147	1	150		142
27	Co	111	3	138[c]		124	86	Rn	142	1, 2, 4	150		
28	Ni	110	2, 3	124		120	87	Fr	223	1	260		
29	Cu	112	1, 2	132		112	88	Ra	201	2	221		
30	Zn	118	1, 2	122		120	89	Ac	186	3	215		
31	Ga	124	3	122		124	90	Th	175	4	206		165
32	Ge	121	4	120	122	122	91	Pa	169	5	200		
33	As	121	3	119	121	123	92	U	170	3, 6	196		160
34	Se	116	2	120	117	119	93	Np	171	4	190		
35	Br	114	1	120	114	114	94	Pu	172	3, 4	187		
36	Kr	117	1, 2	116			95	Am	166	3	180		
37	Rb	210	1	220		212	96	Cm	166	3	169		
38	Sr	185	2	195		189	97	Bk	168	3			
39	Y	163	3	190		162	98	Cf	168	3			
40	Zr	154	3, 4	175		153	99	Es	165	3			
41	Nb	147	4, 5	164		136	100	Fm	167	3			
42	Mo	138	2, 6	154		133	101	Md	173	3			
43	Tc	128	5	147		134	102	No	176	2			
44	Ru	125	4	146		131	103	Lr	161	3			
45	Rh	125	3	142		127	104	Rf	157	4			
46	Pd	120	2	139		130	105	Db	149	3, 5			
47	Ag	128	1	145		127	106	Sg	143	3, 6			
48	Cd	136	1, 2	144		136	107	Bh	141	3, 5			
49	In	142	3	142		145	108	Hs	134	4			
50	Sn	140	4	139	140	140	109	Mt	129	3			
51	Sb	140	3	139	141	143	110	Ds	128	2, 3			
52	Te	136	2	138	137	140	111	Rg	121	1			
53	I	133	1	139	133	133	112	Cn	122	1			
54	Xe	131	1, 2, 4	140			113		136	3			
55	Cs	232	1	244		231	114	Fl	143	4			
56	Ba	196	2	215		197	115		162	3			
57	La	180	3	207		169	116	Lv	175	2			
58	Ce	163	3	204			117		165	1			
59	Pr	176	3	203			118		157	1, 2, 4			

[a]Here CN is the typical coordination number used in PW.[1]. [b]For sp^3-hybridized carbon. Their r_1(C) for sp^2 and sp-hybridized carbon are 73 and 69 pm, respectively. [c]Average of low-spin and high-spin values.

dx.doi.org/10.1021/jp5065819 | J. Phys. Chem. A 2015, 119, 2326–2337

Table 3. Comparisons of Present Double-Bond Radii, r_2 ("PW",[2] pm) with Some Earlier Values

Z	E	PW	Pauling[5]	Batsanov[19]	Z	E	PW	Pauling[5]	Batsanov[19]
3	Li	124	–	–	58	Ce	137	–	–
4	Be	90	–	–	59	Pr	138	–	–
5	B	78	–	76	60	Nd	137	–	–
6	C	67	66.7	67	61	Pm	135	–	–
7	N	60	–	62.5	62	Sm	134	–	–
8	O	57	–	60.5	63	Eu	134	–	–
9	F	59	–	54	64	Gd	135	–	–
10	Ne	96	–	–	65	Tb	135	–	–
11	Na	160	–	–	66	Dy	133	–	–
12	Mg	132	–	–	67	Ho	133	–	–
13	Al	113	–	128	68	Er	133	–	–
14	Si	107	107	107	69	Tm	131	–	–
15	P	102	100	100	70	Yb	129	–	–
16	S	94	94	94	71	Lu	131	–	–
17	Cl	95	89	89	72	Hf	128	–	–
18	Ar	107	–	–	73	Ta	126	–	137
19	K	193	–	–	74	W	120	–	126
20	Ca	147	–	–	75	Re	119	–	119
21	Sc	116	–	–	76	Os	116	–	121
22	Ti	117	–	123	77	Ir	115	–	122
23	V	112	–	–	78	Pt	112	–	122
24	Cr	111	–	124	79	Au	121	–	–
25	Mn	105	–	122	80	Hg	142	–	–
26	Fe	109	–	117	81	Tl	142	–	–
27	Co	103	–	116	82	Pb	135	–	–
28	Ni	101	–	114	83	Bi	141	–	141
29	Cu	115	–	–	84	Po	135	–	–
30	Zn	120	–	–	85	At	138	–	–
31	Ga	117	–	113	86	Rn	145	–	–
32	Ge	111	112	113	87	Fr	218	–	–
33	As	114	111	111	88	Ra	173	–	–
34	Se	107	107	108	89	Ac	153	–	–
35	Br	109	104	104	90	Th	143	–	–
36	Kr	121	–	–	91	Pa	138	–	–
37	Rb	202	–	–	92	U	134	–	–
38	Sr	157	–	–	93	Np	136	–	–
39	Y	130	–	–	94	Pu	135	–	–
40	Zr	127	–	–	95	Am	135	–	–
41	Nb	125	–	136	96	Cm	136	–	–
42	Mo	121	–	–	97	Bk	139	–	–
43	Tc	120	–	–	98	Cf	140	–	–
44	Ru	114	–	117	99	Es	140	–	–
45	Rh	110	–	120	100	Fm	–	–	–
46	Pd	117	–	121	101	Md	139	–	–
47	Ag	139	–	–	102	No	159	–	–
48	Cd	144	–	–	103	Lr	141	–	–
49	In	136	–	–	104	Rf	140	–	–
50	Sn	130	130	130	105	Db	136	–	–
51	Sb	133	131	133	106	Sg	128	–	–
52	Te	128	127	128	107	Bh	128	–	–
53	I	129	123	123	108	Hs	125	–	–
54	Xe	135	–	–	109	Mt	125	–	–
55	Cs	209	–	–	110	Ds	116	–	–
56	Ba	161	–	–	111	Rg	116	–	–
57	La	139	–	–	112	Cn	137	–	–

much above experiment. Note that the average CN used in their fit was much larger than the present ones.

Metal–Metal Bonds. An–TM. Gardner et al.[43] report experimental unbridged U–Ru distances of 299–309 pm. The present r_1 give 295 pm, compared to the Cordero et al.[7] value of 342 pm. The difference can be rationalized by the typically larger CN in Cordero et al.'s data set. The same level of agreement was obtained for the U–Re bonds of Gardner et al.[44] For Th–Fe,

dx.doi.org/10.1021/jp5065819 | J. Phys. Chem. A 2015, 119, 2326–2337

Table 4. Comparisons of Present Triple-Bond Radii, r_3 ("PW", [3] pm) with Some Earlier Values

Z	E	PW	Pauling[5]	Batsanov[19]	Z	E	PW	Pauling[5]	Batsanov[19]
4	Be	85			50	Sn	132	–	–
5	B	73	–	68	51	Sb	127	–	117
6	C	60	60.3	60	52	Te	121	–	–
7	N	54	–	55	53	I	125	–	–
8	O	53	–	–	54	Xe	122	–	–
9	F	53	–	–	56	Ba	149	–	–
12	Mg	127	–	–	57	La	139	–	–
13	Al	111	–	–	58	Ce	131	–	–
14	Si	102	100	100	59	Pr	128	–	–
15	P	94	93	93	64	Gd	132	–	–
16	S	95	87	87	71	Lu	131	–	–
17	Cl	93	–	–	72	Hf	122	–	–
18	Ar	96	–	–	73	Ta	119	–	–
20	Ca	133	–	–	74	W	115	–	112
21	Sc	114	–	–	75	Re	110	–	113
22	Ti	108	–	97	76	Os	109	–	108
23	V	106	–	119	77	Ir	107	–	–
24	Cr	103	–	111	78	Pt	110	–	–
25	Mn	103	–	–	79	Au	123	–	–
26	Fe	102	–	–	81	Tl	150	–	–
27	Co	96	–	–	82	Pb	137	–	–
28	Ni	101	–	–	83	Bi	135	–	133
29	Cu	120	–	–	84	Po	129	–	–
31	Ga	121	–	103	85	At	138	–	–
32	Ge	114	–	106	86	Rn	133	–	–
33	As	106	–	105	88	Ra	159	–	–
34	Se	107	–	–	89	Ac	140	–	–
35	Br	110	–	–	90	Th	136	–	–
36	Kr	108	–	–	91	Pa	129	–	–
38	Sr	139	–	–	92	U	118	–	–
39	Y	124	–	–	93	Np	116	–	–
40	Zr	121	–	–	104	Rf	131	–	–
41	Nb	116	–	–	105	Db	126	–	–
42	Mo	113	–	113	106	Sg	121	–	–
43	Tc	110	–	109	107	Bh	119	–	–
44	Ru	103	–	–	108	Hs	118	–	–
45	Rh	106	–	–	109	Mt	113	–	–
46	Pd	112	–	–	110	Ds	112	–	–
47	Ag	137	–	–	111	Rg	118	–	–
49	In	146	–	–	112	Cn	130	–	–

Th−Ru, and further U−Ru and U−Re bonds, see Oelkers et al.[45] See also the section 3.5.

Superheavies. The diatomic $(E117)_2$ has a calculated R of 352 pm.[46] Half of this is 176 pm, compared to our fitted r_1 of 165 pm.

3.4. Double-Bond Radii. *B═B Bonds.* The present $2r_2(B)$ is 156 pm. Brand et al.[29] quote their species **28** with 151 pm.

P═S. An accurate gas-phase microwave value of 192.87 pm[47] is available for the r_e(P═S) of the bent H−P═S. The r_2 would predict 196 pm. In the carboranyl P(V) complex **9** of Popescu et al.,[48] the P═S distance is 194.2 pm. Their P═Se distance of 209.8 pm in their **15** also is head-on with the Σr_2 of 209 pm. The P═O in their **3, 5** is closer to the Σr_3 of 147 pm. Of the valence isoelectronic systems to H−P═S, the P═O of HPO, 148.00(9),[49] also is between the sum of r_3 and r_2. For the more electronegative central atom N, the bond lengths of HNO and HNS, 121.2 and 157.0 pm, respectively, are on the long side of Σr_2.

Ge═O. The first germanone, analogous to a ketone, was synthesized by Li et al.[50] The observed Ge═O bond length is 164.68(5) pm. The r_2 would predict 168 pm.

Mo═C. Examples on such bonds of around 188−193 pm are quoted in the review of Odom.[51] The Σr_2 is 188 pm.

M═P. For a review on the double bonds in [L_nTM═P—R] systems, see the review by Aktas et al.[52] As an example, for TM = Ti, Nb, Ta the R(TM═P) are experimentally 216.4, 227.3, and 231.7 pm while the r_2 radii yield 219, 227, and 228 pm, respectively.

Actinides. The primary data in the present r_2 and r_3 fits had second-period or TM ligands (C−O, Ir−Pt). Interestingly, if the third-period analogues P and S would be used, an NBO orbital analysis shows well-developed multiple bonds, but their effective radii, r(An), are larger than in our tables. For some examples, see section 3.5.

Also for FB═ThF_2 the r_2(Th) yields a B═Th bond of 221 pm, compared to the CASPT2 R(B═Th) of 245 pm by Wang et al.[53] For the borylene complexes, FB═MF_2, M = Ti, Zr, Hf, the CASPT2 calculations give 209.4, 222.0, and 215.6 pm,[54] and the r_2 195, 205, and 206 pm, respectively.

In H_2AnS, An = Th, U, the An−S distances are not far from Σr_2. However, instead of a single, well-defined π bond, there were

dx.doi.org/10.1021/jp5065819 | J. Phys. Chem. A 2015, 119, 2326−2337

two weakish π bonds.[55] The An−H bond lengths match well the Σr_1. In N≡U═NH the N≡U and U═NH bonds match well Σr_3 and Σr_2, respectively.[56] The NUN bond length also fits r_3.

3.5. Triple-Bond Radii. *B−B.* The observed matrix species OCB−BCO[57] and gas-phase species $[OBB-BBO]^{2-}$[58] have a calculated central triple bond length near the 2 r_3 of 146 pm. For a further review, see Braunschweig and Dewhurst.[59] A theoretical analysis was given by Ducati et al.,[60] including NNB−-BNN.

B−O and B−X. The data set for r_3 included the free BO^- ion. The r_3 would predict an R of 126 pm. Bettinger et al.[61] report for MeBO calculated and experimental B−O bond lengths of 121.3 and 120.1 pm, respectively. Further examples at 120−123 pm are quoted by Brand et al.[29] In the series B−X, Al−X, the Ga−X, X = F, Cl, Br have bond lengths comparable with the Σr_3.[62] Thus, the isoelectronic analogy from XY = N_2 to CO to BF seems to have a broad range of applicability, both for these free diatomics and for them as ligands in R−XY.

N≡S Bonds. The experimental structure of N≡SF_3 has a bond length of 140 pm.[63] The Σr_3 is 149 pm.

Fourth-Period E≡E Bonds. For a review and analysis of this topic, such as the Ge≡Ge germyne bonds, see Ploshnik et al.[64]

Mo≡S. The experimental bond length in systems such as S≡MoF_4 or 206−207 pm[65] is close to the Σr_3 of 208 pm. Since a visual inspection of the molecular orbitals shows a $\sigma^2\pi^4$ structure, there is no reason not to call the Mo≡S bond or its analogues triple ones.

Further Triple Bonds between Transition Metals and Group-14 Elements. Hayes et al.[66] report Os≡Si bonds of ≥217 pm (Σr_3 = 211 pm). Filippou et al.[67] observe an Mn≡Sn of 234 pm and mention that the Σr_3 is 235 pm.

TM Terminal Oxo Compounds. Zhu et al.[68] unequivocally classify the O≡Ti and O≡Cr bonds as triple bonds.

Fe≡N. A typical range of experimental bond lengths is 150−155, 161, and 157 pm for Fe(IV), Fe(V), and Fe(VI), respectively.[69] The triple bond radii give 156 pm.

Rh≡P. As noted in our paper,[3] our r_3 predict for the diatomic RhP 200 pm, close to our DFT bond length of 198 pm, while a reported experimental value was 186 pm.[70] It turned out that this experiment had missed rotational levels and the corrected experimental R_0 is 200.2(20) pm.[71] For the valence isoelectronic IrP($X\ ^1\Sigma_g$), the Σr_3 and experimental R_0[72] are 201 and 199 pm, respectively.

Mo≡Ge. Hicks et al.[73] synthesized a germylyne species (their **3**), $(CO)_2$(cp)Mo≡Ge−N(Ar)(R) with a Mo−Ge distance of 228.1 pm. They also quote several compounds with analogous Mo≡Ge bonds. The present triple-bond radii predict 227 pm.

Tc−Tc Bonding. The three Tc≡Tc bonds in the D_{3h} systems $Tc_6Cl_{12}^-$, discussed by Wheeler and Hoffmann,[74] have a bond length of 221 pm, compared to the Σr_3 of 220 pm. The six single Tc−Tc bonds in the triangular faces are 257 pm while the r_1 would predict 256 pm.

La−Lu. The main covalent bonding orbitals of the lanthanides are, in this order of importance, the (5d, 6s, 6p); see for instance ref 75. Nothing prevents these metals from making single, double,[76,77] or triple covalent bonds, in a rough agreement with the present r_1, r_2, and r_3, respectively. The same is true for the dsp orbitals of (Sc, Y). An example is the Ce≡O bond[78] in a Ce(IV) complex, where experiments yield 186 and the r_3 184 pm. For examples on r_1 cases, see Table 5. Note that the experimental CN tend to be larger than those assumed in the input data for determining our r_1 in Table 2.

W. A recent example on r_3(W) are the intramolecular bond lengths[82] inside the W−W≡O groups in $[W_2O(2,2'\text{-dipyridylamide})_4]^{2+}$. Both the W−W and W−O distances conform to the present r_3; see Table 6. Pandey and Patidar[84] calculate W≡Ge and W≡Pb distances of 232 and 258 pm, compared to the r_3 prediction of 229 and 252 pm, respectively.

Table 5. Further Tests of the Present Covalent Radii, TM = Transition-Metal, M = Main-Group Element, Ln = Lanthanide, and An = Actinide

class	bond	expt	Σr_1
Ln−TM	Lu−Ru[a]	299.5	287
	Y−Re[a]	296.2	294
	Yb−Fe[b]	298.9	286
An−TM[a]	Th−Ru	302.8	300
	U−Re	304.8	301
Ln−M[a]	Y−Ga	317.6	287
	Yb−Si	303.2	286
An−M[a]	U−Ga	322.1/329.8	294
	U−Ga	306.5/308.0	294
	U−Sn	316.6	310
	U−Si	309.1	286
TM−M	Fe−Mg[c]	263.3	255
	Fe−Ca[b]	301.8	287

[a]See ref 79. [b]See ref 80. [c]See ref 81.

Table 6. Further Tests on the Present Triple-Bond Radii

X	bond	expt	Σr_3	ref
W	W−W	272	274	82
	W−O	169.6	168	82
U	U−O	174	171	83
	U−S	239	213	83
	U−Se	255	225	83

Pt−Tl. A further example on such a triple bond was produced by Purgel et al.:[85] experimental bond length, 267 pm; Σr_3, 260 pm.

Au. The r_3 of Au is 123 pm, much longer than that of 110 pm for Pt or preceding elements. The input data for Au in ref 3 comprised the 14e species AuB, AuC^+, AuN^{2+}, AuAl, $AuSi^+$, and AuGa, while AuIn and AuTl had to be excluded. This suggests that we are at the edge of multiple bonding. For the 12e species $AuBe^+$ a CASPT2 calculation[86] gives an R_e of 198.3 pm, which would yield an r_3(Au) of 198 − 85 = 113 pm, the positive total charge also increasing multiple covalent bonding. Note that $AuBe^+$ achieves a triple bond with 2e less than AuC^+.

Th≡S. The radii would predict a bond length of 231 pm for diatomic ThS. A recent measurement by Le et al.[87] gives 234.36(7) pm.

An≡ Bonds. The diatomic Th≡O and members of the uranyl isoelectronic series were used as input data when deriving the r_3 values.[3] The ThO is a "heavy CO" and shares with it the $\sigma^2\pi^4$ electron configuration; see the 8e case in Figure 3. The uranyl-type series included members of the monosubstituted O≡U≡Ir^+ series. The latter isoelectronic family was predicted[88] and subsequently observed.[89] The triple-bond character of the uranyl ion OUO^{2+} is explained by its electron configuration[90]

$$\pi_g^4\pi_u^4\sigma_g^2\sigma_u^2 \qquad (3)$$

all 12 electrons bonding.

Perhaps less intuitive are the triple O≡AnF_2 bonds, found for the case An = Th or U by Gong et al.[91] They are supported by the

dx.doi.org/10.1021/jp5065819 | J. Phys. Chem. A 2015, 119, 2326−2337

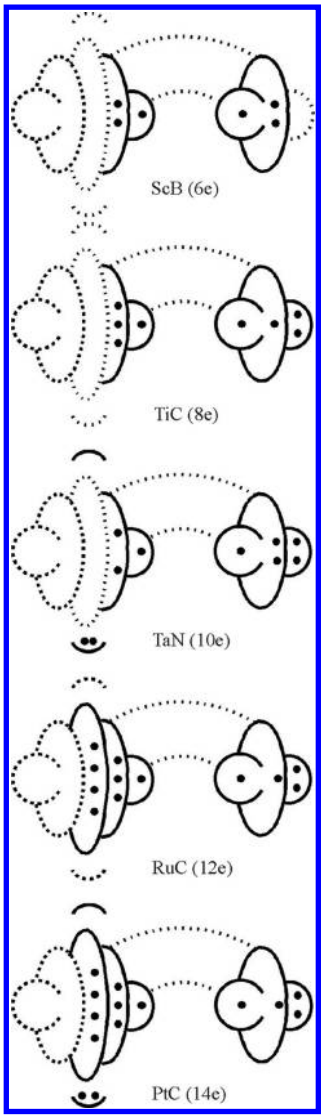

Figure 3. Formation of a $\sigma^2\pi^4$ triple bond in diatomics with 6−14 valence electrons. For explanations, see the text. Adapted with permission from ref 3. Copyright 2005 Wiley-VCH.

calculated NBO structures. For An = Th the calculated bond length of 189 pm is head-on with the r_3 prediction of 189 pm. For An = U the QC value of 183 is between the sums of the triple- and double-bond radii of 171 and 191 pm, respectively.

For the $[O-U-E]^{2+}$ moiety the E═O result agrees with the r_3 radii, but the experimental E = S, Se distances[83] are much longer than those predicted by the triple-bond radii; see Table 6.

Andrews et al.[92] saw the P≡UF_3 molecule in matrix specroscopy. The calculated CASPT2 U−P distance is 240 pm, compared with Σr_3 = 212 pm. Yet the NBO orbitals show that a $\sigma^2\pi^4$ triple bond would be there. The PUP $X^3\Phi_u$ ground-state bond length is calculated to be 236 pm.[93] All this suggests different bonding modes for uranium multiple bonds to second- and third-period elements; see Table 7. For thorium, the same r_3(Th) fits all ligands. Possibly this reflects a loss of 5f bonding in the larger, third-period (n = 3) ligands for U. For Th the 5f-bonding is smaller anyway; as shown in Figure 1 of ref 94, the 5f is crossing the 6d at Pa.

A further example on an $(L\text{-})_3U{\equiv}N$ bond is the recent uranium nitride **7** of King et al.[95] The experimental triple-bond length is 179.9(7) pm, compared with the Σr_3 of 172 pm.

Table 7. Some Cases Where the Present Multiple-Bond Radii Do or Do Not Work, Second-Period Elements "2" = C, N, O; Third-Period Elements "3" = P, S; Transition Metals TM = Ir, Pt; Actinides An = Th, Pa, U[a]

class	species	expt/calc	Σr_n	works?
2-An-2′	$OPaO^+$	181.2	182	yes
	$[O{\equiv}U{\equiv}O]^{2+}$	171.5	171	yes
	$ONpO^{3+}$	168.2	169	yes
	NUN	168[90]	172	yes
2-An−TM	NU≡Ir	218.4	225	yes
	N≡UIr	174	172	yes
2-An	ThO	184.03	189	yes
TM−An	PtTh	250	246	yes
3-An	ThS	234.36(7)	231	yes
2-An-3	$OU{\equiv}S^{2+}$	239	213	no
3-An-3	PU≡P	236	212	no
3-AnF_3	P≡UF_3	240	212	no

[a]. Unless otherwise stated, the data sources are given in refs 2 and 3 or in the text.

Beyond Triple Bonds. This issue was discussed in ref 1. A further example is the diatomic $X^1\Sigma^+$ ZrFe.[96] The experimental r_0 of 187.685 pm is far below the Σr_3 of 223 pm.

Note here that Wang et al.[97] calculate for the coaxial dibenzene dimetal compounds, b−M−M−b, M = Fe, Mn, and Cr, b = C_6H_6, the M−M distances of 195, 173, and 167 pm, much below the triple-bond distances Σr_3 of 204, 206, and 206 pm (radii), respectively. In fact, a large amount of literature exists on such multiple bonds.

Same Bond Order with a Different Number of Valence Electrons. As seen in Figure 3, a triple bond can be achieved with a different number of valence electrons, the extra electrons in the 8e to 14e cases going to lone-pair σ, doughnut σ, and δ orbitals, in this approximate order, respectively.

Recall here the bonding analogy between terminal ≡O and ≡Pt bonds, or between ≡N and ≡Ir bonds. Examples are the experimentally known CO analogue CPt or the predicted[88] and found[89] OUN^+ analogue $OUIr^+$. Recall also the known RhN, IrN, and IrP, used in our r_3 fit.

3.6. Tetrahedral Radii. *Mixed Crystals and Vegard's Law.* Vegard's law[98] states that, for fairly similar atomic radii, the lattice parameters in an alloy change linearly from one limit to the other limit. A recent example would be the semiconductor $Sc_{1-x}In_xP$, ref 99, with the limits ScP and InP, both taken with a ZnS structure. Some deviations from linearity are found.

Tetrahedral Crystal Radii versus Single-Bond Radii. For the group-14 elements C, Si, Ge, and Sn, the r_T and the r_1 would be expected to be close. Indeed, the two sets are (77.3, 117.6, 122.5, 140.0) and (75, 116, 121, 140) pm, respectively. For their group 11−13 or group 15−17 neighbors, the molecular and tetrahedral solid-state surroundings are different, and no close similarity should be expected. An early comparison between tetrahedral molecular and crystal radii for seven elements, Li−F, was given by Beagley.[100]

Number of Components and Possible Crystal Structures. For one or two elements, we can have the ZnS (zincblende, ZB) or the wurtzite (hexagonal diamond, lonsdaleite) structures, where both atoms have a tetrahedral site symmetry. An average of the R is taken in the latter case. Note, moreover, the possibility of layered superlattices, such as Si_3C or SiC_3.[101] For three components, the $CuES_2$, $CuESe_2$, and $AgESe_2$ chalcopyrites E = Al, In, Ga were used for fitting the r_T in ref 4. As a further test

dx.doi.org/10.1021/jp5065819 | J. Phys. Chem. A 2015, 119, 2326−2337

there, the four-component kesterite or stannite structures, such as Cu_2ZnSnS_4 or $Cu_2ZnSnSe_4$, were used. A thorough test of various ionic or covalent radii, including the present r_T, on over 40 wurz-kesterite compounds was carried out by Aitken's group.[102] Three of the compounds were newly synthesized. All of these could be called "diamond-like semiconductors (DLS)". For further references, see Brunetta et al.[102] Another term is "adamantine" compounds.[103] Some further possible tests are $Cu_2Mn_{1-x}Co_xSnS_4$[103] and $Cd_{1-x}Zn_xS$.[104]

Influence of Oxidation State. Tin is the next to be examined. The derivation of the r_T(Sn) of 140.0 pm in our r_T paper[4] was based on gray tin, Sn(0). In the ZB SnS[105] we have Sn(II), and it is then perhaps natural that the resulting r_T of Sn(II), 148.9 pm, would differ from it. The r_1(Sn) of 140 pm is derived from a six-point data set including five Sn(IV) compounds and the Sn(0) gray tin.

BBi and Inverted Cation−Anion Roles. Madouri and Ferhat[106] calculate for the ZB III−V compound BBi an LDA R of 234.5 pm, head-on with the r_T prediction of 234.2 pm. They moreover find inverted cation−anion roles in this strongly relativistic compound.

Some Outliers. As summarized in ref 4, the solid SiC is an outlier, with anomalously short Si−C bonds. Both ionic contributions, a small 2p-shell core repulsion from Si, or possible 3d contributions have been suggested as possible reasons. For a study on the various phases of the Si/C system, see Gao et al.[101] We note that the isoelectronic nearest neighbor AlN also has anomalously short bonds.

Qualitatively, a similar trend is found for the pseudocubic solids A_3B_4 where A is a group-4 element, C to Sn, and B is a group-15 element, N to As. A prototype compound is C_3N_4. Lü and Zheng[107] find that the computed combinations Si−N, Ge−N, and Sn−N are "short", while the other cases C−N, C−P, Si−P, Ge−P, Sn−P, C−As, Si−As, G−As, and Sn−As agree well with the r_T. Note that here only the A atom is tetrahedrally surrounded while the B atom has CN = 3, and a lone-pair occupies the fourth direction. The physical explanation of these anomalies would be interesting.

4. DISCUSSION

Relation to Ionization Potentials. DeKock et al.[108] and Agmon[109] have made attempts to relate the covalent radii r_A of an atom A to its experimental ionization potential (IP) $I_A = I^*$:

$$r_A = r_H n^* \sqrt{\frac{I_H}{I^*}} \tag{4}$$

where r_H is the hydrogenic radius, a_0, and n^* is the effective principal quantum number yielding the IP I^* for element A. The results from eq 4 were compared with those of Cordero et al.[7] and roughly agreed with them. The earlier literature on the relation of atomic radii to the IP ranges from Bohórquez and Boyd[110] back to Slater.[111] We conclude that this approach gives useful semiquantitative estimates for covalent radii.

Relation to Electron Localization Functions, ELF. B−N bonds can range from single to triple. Berski et al.[28] related, as said in section 3.2., their bond lengths to the ELF populations.

5. CONCLUSION

Our key conclusion is that one can get surprisingly far with the simple, additive formula (1), with one "covalent radius" per element, for the particular bonding situation. The agreement of the predicted R with experiment is good, provided that the A−B bond is not too ionic, nor the coordination numbers of the two atoms too different from the input data. What goes in, comes out. Moreover, note the exclusion of TM−X single bonds between transition metals and electronegative elements, such as halides, due to their π back-bonding and consequent partial multiple-bond character.

A number of anomalous nooks and crannies are identified; see sections 3.2 and 3.5.

AUTHOR INFORMATION

Corresponding Author

*E-mail: Pekka.Pyykko@helsinki.fi. Tel.: +358 2941 50171.

Notes

The authors declare no competing financial interest.

ACKNOWLEDGMENTS

Table of Content and Abstract graphics are adapted with permission from *Chem.—Eur. J.* **2005**, *11*, 3511. Copyright 2005 Wiley-VCH.

REFERENCES

(1) Pyykkö, P.; Atsumi, M. Molecular single-bond covalent radii for elements 1−118. *Chem.—Eur. J.* **2009**, *15*, 186−197.
(2) Pyykkö, P.; Atsumi, M. Molecular double-bond covalent radii for elements Li-E112. *Chem.—Eur. J.* **2009**, *15*, 12770−12779.
(3) Pyykkö, P.; Riedel, S.; Patzschke, M. Triple-bond covalent radii. *Chem.—Eur. J.* **2005**, *11*, 3511−3520.
(4) Pyykkö, P. Refitted tetrahedral covalent radii for solids. *Phys. Rev. B* **2012**, *85*, No. 024115.
(5) Pauling, L. *The Nature of the Chemical Bond*, 3rd ed.; Cornell University Press: Ithaca, NY, USA, 1960.
(6) Slater, J. C. Atomic radii in crystals. *J. Chem. Phys.* **1964**, *41*, 3199−3204.
(7) Cordero, B.; Gómez, V.; Platero-Prats, A. E.; Revés, M.; Echeverría, J.; Cremades, E.; Barragán, F.; Alvarez, S. Covalent radii revisited. *Dalton Trans.* **2008**, 2832−2838.
(8) Mantina, M.; Valero, R.; Cramer, C. J.; Truhlar, D. G. Atomic radii of the elements. *CRC Handbook of Chemistry and Physics*; CRC Press: Boca Raton, FL, USA, 2010; pp 9-49−9-50.
(9) Bragg, W. L. The arrangement of atoms in crystals. *Philos. Mag.* **1920**, *40*, 169−189.
(10) Wasastjerna, J. A. On the radii of ions. *Soc. Sci. Fenn., Commentat. Phys.-Math.* **1923**, *1* (No. 38), 1−25.
(11) Shannon, R. D.; Prewitt, C. T. Effective ionic radii in oxides and fluorides. *Acta Crystallogr., Sect. B: Struct. Crystallogr. Cryst. Chem.* **1969**, *25*, 925−946.
(12) Shannon, R. D. Revised effective ionic radii and systematic studies of interatomic distances in halides and chalcogenides. *Acta Crystallogr., Sect. A: Cryst. Phys., Diffr., Theor. Gen.* **1976**, *32*, 751−767.
(13) Gibbs, G. V.; Ross, N. L.; Cox, D. F.; Rosso, K. M.; Iversen, B. B.; Spackman, M. A. Bonded radii and the contraction of the electron density of the oxygen atom by bonded interactions. *J. Phys. Chem. A* **2013**, *117*, 1632−1640.
(14) Liu, J.-B.; Schwarz, W. H. E.; Li, J. On two different objectives of the concepts of ionic radii. *Chem.—Eur. J.* **2013**, *19*, 14758−14767.
(15) Lang, P. F.; Smith, B. C. Ionic radii for Group 1 and Group 2 halide, hydride, fluoride, oxide, sulfide, selenide and telluride crystals. *Dalton Trans.* **2010**, *39*, 7786−7791.
(16) Schomaker, V.; Stevenson, D. P. Some revisions of the covalent radii and the additivity rule for the lengths of partially ionic single covalent bonds. *J. Am. Chem. Soc.* **1941**, *63*, 37−40.
(17) Lang, P. F.; Smith, B. C. Electronegativity effects and single covalent bond lengths of molecules in the gas phase. *Dalton Trans.* **2014**, *43*, 8016−8025.
(18) Wells, A. F. Bond lengths in some inorganic molecules and complex ions. *J. Chem. Soc.* **1949**, 55−67.

(19) Batsanov, S. S. *Experimental Foundations of Structural Chemistry*; Moscow University Press: Moscow, 2008; 542 pp.
(20) Ivanova, M.; Stein, A.; Pashov, A.; Knöckel, H.; Tiemann, E. The $X\,^1\Sigma^+$ state of LiRb studied by Fourier-transform spectroscopy. *J. Chem. Phys.* **2011**, *134*, No. 024321.
(21) Ferber, R.; Klincare, I.; Nikolayeva, O. The ground electronic state of KCs studied by Fourier transform spectroscopy. *J. Chem. Phys.* **2008**, *128*, No. 244316.
(22) Sanderson, R. T. *Inorganic Chemistry*; Reinhold: New York, 1967; p 74.
(23) Haaland, A.; Shorokhov, D. J.; Tutukin, A. V.; Volden, H. V.; Swang, O.; McGrady, G. S.; Kaltsoyannis, N.; Downs, A. J.; Tang, C. Y.; Turner, J. F. C. Molecular structures of two metal tetrakis-(tetrahydroborates), $Zr(BH_4)_4$ and $U(BH_4)_4$: Equilibrium conformations and barriers to internal rotation of the triply bridging BH_4 groups. *Inorg. Chem.* **2002**, *41*, 6646−6655.
(24) Ravnsbæk, D. B.; Frommen, C.; Reed, D.; Filinchuk, Y.; Sørby, M.; Hauback, B. C.; Jakobsen, H. J.; Book, D.; Besenbacher, F.; Skibsted, J.; et al. Structural studies of lithium zinc borohydride by neutron powder diffraction, Raman and NMR spectroscopy. *J. Alloys Compd.* **2011**, *509S*, S698−S704 , and references therein..
(25) Wells, A. F. *Structural Inorganic Chemistry*; Oxford University Press: Oxford, U. K., 1984.
(26) Hudgens, J. W.; Johnson, R. D., III; Tsai, B. P.; Kafafi, S. A. Experimental and ab initio studies of electronic structures of the CCl_3 radical and cation. *J. Am. Chem. Soc.* **1990**, *112*, 5763−5772.
(27) Krebs, B.; Hamann, W. Ortho-thioborates and ortho-selenoborates: Synthesis, structure and properties of Tl_3BS_3 and Tl_3BSe_3. *J. Less-Common Met.* **1988**, *137*, 143−154.
(28) Berski, S.; Latajka, Z.; Gordon, A. J. On the multiple B-N bonding in boron compounds using the topological analysis of electron localization function (ELF). *New J. Chem.* **2011**, *35*, 89−96.
(29) Brand, J.; Braunschweig, H.; Sen, S. S. B═B and B≡E (E = N and O) multiple bonds in the coordination sphere of late transition metals. *Acc. Chem. Res.* **2014**, *47*, 180−191.
(30) Pyykkö, P. Ab initio predictions for new chemical species. *Phys. Scr.* **1990**, *T33*, 52−53.
(31) Pyykkö, P. Ab initio study of the bonding trends among cyanaminophosphates, $[PO_n(NCN)_{4-n}]^{3-}$, and related systems. *Chem.—Eur. J.* **2000**, *6*, 2145−2151.
(32) Lindh, R.; Kraemer, W. P.; Kämper, M. On the thermodynamic stability of ArO_4. *J. Phys. Chem. A* **1999**, *103*, 8295−8302.
(33) Xiong, X.-G.; Pyykkö, P. Unbridged Au(II)-Au(II) bonds are theoretically allowed. *Chem. Commun. (Cambridge, U. K.)* **2013**, *49*, 2103−2105.
(34) Batsanov, S. S. H_2: An archetypal molecule or an odd exception? *Struct. Chem.* **1998**, *9*, 65−68.
(35) Robinson, E. A.; Johnson, S. A.; Tang, T.-H.; Gillespie, R. J. Reinterpretation of the lengths of bonds to fluorine in terms of an almost ionic model. *Inorg. Chem.* **1997**, *36*, 3022−3030.
(36) Vojteer, N.; Sagawe, V.; Stauffer, J.; Schroeder, M.; Hillebrecht, H. $LiB_{12}PC$, the first boron-rich metal boride with phosphorus—Synthesis, crystal structure, hardness, spectroscopic investigations. *Chem.—Eur. J.* **2011**, *17*, 3128−3135.
(37) Balasanthiran, V.; Chisholm, M. H.; Durr, C. B. On the molecular structure and bonding in a lithium bismuth porphyrin complex: $LiBi(TPP)_2$. *Angew. Chem., Int. Ed.* **2014**, *53*, 1594−1597.
(38) Díaz-Torrejón, C. C.; Kaplan, I. G. Many-body forces and stability of the alkaline-earth tetramers. *Chem. Phys.* **2011**, *381*, 67−71.
(39) Ascik, P. N.; Wilke, J. J.; Simmonett, A. C.; Yamaguchi, Y.; Schaefer, H. F., III. The beryllium tetramer: Profiling an elusive molecule. *J. Chem. Phys.* **2011**, *134*, No. 074110.
(40) Traut, S.; Hähnel, A. P.; von Hänisch, C. Dichloro organosilicon bismuthanes as precursors for rare compounds with a bismuth-pnictogen or bismuth-tellurium bond. *Dalton Trans.* **2011**, *40*, 1365−1371.
(41) Thiele, G.; Krüger, T.; Dehnen, S. $K_4[PbSe_4]\cdot en\cdot NH_3$: A non-oxide, non-halide inorganic lead(IV) compound. *Angew. Chem., Int. Ed.* **2014**, *53*, 4699−4703.
(42) Zeckert, K.; Griebel, J.; Kirmse, R.; Weiss, M.; Denecke, R. Versatile reactivity of a lithium tris(aryl)plumbate(II) towards organo-lanthanoid compounds: Stable lead-lanthanoid-metal bonds or redox processes. *Chem.—Eur. J.* **2013**, *19*, 7718−7722.
(43) Gardner, B. M.; Patel, D.; Cornish, A. D.; McMaster, J.; Lewis, W.; Blake, A. J.; Liddle, S. T. The nature of unsupported uranium-ruthenium bonds: A combined experimental and theoretical study. *Chem.—Eur. J.* **2011**, *17*, 11266−11273.
(44) Gardner, B. M.; McMaster, J.; Moro, F.; Lewis, W.; Blake, A. J.; Liddle, S. T. An unsupported uranium-rhenium complex prepared by alkane elimination. *Chem.—Eur. J.* **2011**, *17*, 6909−6912.
(45) Oelkers, R.; Butovskii, M. V.; Kempe, R. f-Element—Metal bonding and the use of the bond polarity to build molecular intermetalloids. *Chem.—Eur. J.* **2012**, *18*, 13566−13579.
(46) Liu, W.-J.; Peng, D.-L. Infinite-order quasirelativistic density functional method based on the exact matrix quasirelativistic theory. *J. Chem. Phys.* **2006**, *125*, No. 044102;Erratum: **2006**, *125*, No. 149901.
(47) Halfen, D. T.; Clouthier, D. J.; Ziurys, L. M.; Lattanzi, V.; McGarthy, M. C.; Thaddeus, P.; Thorwirth, S. The pure rotational spectrum of HPS ($\tilde{X}^1$ A′): Chemical bonding in second-row elements. *J. Chem. Phys.* **2011**, *134*, No. 134302.
(48) Popescu, A.-R.; Laromaine, A.; Teixidor, F.; Sillanpää, R.; Kivekäs, R.; Llambias, J. I.; Viñas, C. Uncommon coordination behaviour of P(S) and P(Se) units when bonded to carboranyl clusters: Experimental and computational studies on the oxidation of carboranyl phosphine ligands. *Chem.—Eur. J.* **2011**, *17*, 4429−4443.
(49) Ozeki, H.; Saito, S. Microwave spectra of HPO and DPO: Molecular structure. *J. Mol. Spectrosc.* **2003**, *219*, 306−312.
(50) Li, L.-C.; Fukawa, T.; Matsuo, T.; Hashizume, D.; Fueno, H.; Tanaka, K.; Tamao, K. A stable germanone as the first isolated heavy ketone with a terminal oxygen atom. *Nat. Chem.* **2012**, *4*, 361−365.
(51) Odom, A. L. Conversions between metal-ligand multiple bond (MLMB) types: Carbonyl olefination and other applications. *Dalton Trans.* **2011**, *47*, 2689−2695.
(52) Aktas, H.; Slootweg, J. C.; Lammertsma, K. Nucleophilic phosphinidene complexes: Access and applicability. *Angew. Chem., Int. Ed.* **2010**, *49*, 2102−2113.
(53) Wang, X.-F.; Roos, B. O.; Andrews, L. Matrix infrared spectra and electronic structure calculations of the first actinide borylene: FB═ThF_2. *Chem. Commun. (Cambridge, U. K.)* **2010**, *46*, 1646−1648.
(54) Wang, X.-F.; Roos, B. O.; Andrews, L. Calculations and matrix infrared spectra of terminal borylene complexes FB═MF_2. *Angew. Chem., Int. Ed.* **2010**, *49*, 157−160.
(55) Wang, X.-F.; Andrews, L.; Thanthiriwatte, K. S.; Dixon, D. A. Infrared spectra of H_2ThS and H_2US in noble gas matrixes: Enhanced H-An-S covalent bonding. *Inorg. Chem.* **2013**, *52*, 10275−10285.
(56) Wang, X.-F.; Andrews, L.; Vlaisavljevich, B.; Gagliardi, L. Combined triple and double bonds to uranium: The N≡U═N—H uranimide nitride molecule prepared in solid argon. *Inorg. Chem.* **2011**, *50*, 3826−3831.
(57) Zhou, M. F.; Tsumori, N.; Li, Z. H.; Fan, K. N.; Andrews, L.; Xu, Q. A. OCBBCO: A neutral molecule with some boron−boron triple bond character. *J. Am. Chem. Soc.* **2002**, *124*, 12936−12937.
(58) Li, S. D.; Zhai, H. J.; Wang, L. S. $B_2(BO)_2^{2-}$-diboronyl diborene: a linear molecule with a triple boron-boron bond. *J. Am. Chem. Soc.* **2008**, *130*, 2573−2579.
(59) Braunschweig, H.; Dewhurst, R. D. Single, double, triple bonds and chains: The formation of electron-precise B-B bonds. *Angew. Chem., Int. Ed.* **2013**, *52*, 3574−3583.
(60) Ducati, L. C.; Takagi, N.; Frenking, G. Molecules with all triple bonds: OCBBCO, N_2BBN_2, and $[OBBBBO]^{2-}$. *J. Phys. Chem. A* **2009**, *113*, 11693−11698.
(61) Bettinger, H. F.; Brough, S.; Grunenberg, J. The Lewis acidity of the BO triple bond in methyl(oxo)borane. *Z. Anorg. Allg. Chem.* **2013**, *639*, 1199−1204.
(62) Vidovic, D.; Aldridge, S. Coordination chemistry of group 13 monohalides. *Chem. Sci.* **2011**, *2*, 601−608.

(63) Smith, G. L.; Mercier, H. P. A.; Schrobilgen, G. J. Ennobling an old molecule: Thiazyl trifluoride ($N{\equiv}SF_3$), a versatile synthon for Xe—N bond formation. *Inorg. Chem.* **2011**, *50*, 12359−12373.
(64) Ploshnik, E.; Danovich, D.; Hiberty, P. C.; Shaik, S. The nature of the idealized triple bonds between principal elements and the σ origins of trans-bent geometries—A valence bond study. *J. Chem. Theory Comput.* **2011**, *7*, 955−968.
(65) Nieboer, J.; Mack, J. P.; Mercier, H. P. A.; Gerken, M. Synthesis, characterization, and computational study of $MoSF_4$. *Inorg. Chem.* **2010**, *49*, 6153−6159.
(66) Hayes, P. G.; Xu, Z.-G.; Beddie, C.; Keith, J. M.; Hall, M. B.; Tilley, T. D. The osmium-silicon triple bond: synthesis, characterization, and reactivity of an osmium silylene complex. *J. Am. Chem. Soc.* **2013**, *135*, 11780−11783.
(67) Filippou, A. C.; Ghana, P.; Chakraborty, U.; Schnakenburg, G. Manganese-tin triple bonds. A new synthetic route to the manganese stannylidene complex cation. *J. Am. Chem. Soc.* **2013**, *135*, 11525−11528.
(68) Zhu, J.-F.; Kurahashi, T.; Fujii, H.; Wu, G. Solid-state ^{17}O NMR and computational studies of terminal transition metal oxo compounds. *Chem. Sci.* **2012**, *3*, 391−397.
(69) Smith, J. M.; Subedi, D. The structure and reactivity of iron nitride complexes. *Dalton Trans* **2012**, *41*, 1423−1429.
(70) Li, R.-H.; Balfour, W. J. Electronic structure and bonding in rhodium monophosphide. *J. Phys. Chem. A* **2004**, *108*, 8145−8146.
(71) Balfour, W. J.; Adam, A. G. RhP. Private communication, Jun. 13, 2014.
(72) Adam, A. G.; Downie, L. E.; Granger, A. D.; Grein, F.; Slaney, M. E.; Linton, C.; Tokaryk, D. W. A high resolution visible spectrum of iridium monophosphide. *J. Mol. Spectrosc.* **2010**, *263*, 111−119.
(73) Hicks, J.; Hadlington, T. J.; Schenk, C.; Li, J.-Y.; Jones, C. Utilizing steric bulk to stabilize molybdenum aminogermylyne and amino-germylene complexes. *Organometallics* **2013**, *32*, 323−329.
(74) Wheeler, R. A.; Hoffmann, R. A new magic cluster electron count and metal-metal multiple bonding. *J. Am. Chem. Soc.* **1986**, *108*, 6605−6610.
(75) Xu, W.-H.; Jin, X.; Chen, M.-H.; Pyykkö, P.; Zhou, M.-F.; Li, J. Rare-earth monocarbonyls MCO: Comprehensive infrared observations and a transparent theoretical interpretation for M═Sc; Y; La-Lu. *Chem. Sci.* **2012**, *3*, 1548−1554.
(76) Roos, B. O.; Pyykkö, P. Bonding trends in molecular compounds of lanthanides: The double-bonded carbene cations $LnCH_2^+$, Ln = Sc, Y, La-Lu. *Chem.—Eur. J.* **2010**, *16*, 270−275.
(77) Gregson, M.; Lu, E.-L.; McMaster, J.; Lewis, W.; Blake, A. J.; Liddle, S. T. A cerium(IV)-carbon multiple bond. *Angew. Chem., Int. Ed.* **2013**, *52*, 13016−13019.
(78) So, Y.-M.; Wang, G.-C.; Li, Y.; Sung, H. H.-Y.; Williams, I. D.; Lin, Z.-Y.; Leung, W.-H. A tetravalent cerium complex containing a Ce═O bond. *Angew. Chem., Int. Ed.* **2014**, *53*, 1626−1629.
(79) Vlaisavljevich, B.; Miró, P.; Cramer, C. J.; Gagliardi, L.; Infante, I.; Liddle, S. T. On the nature of actinide- and lanthanide-metal bonds in heterobimetallic compounds. *Chem.—Eur. J.* **2011**, *17*, 8424−8433.
(80) Blake, M. P.; Kaltsoyannis, N.; Mountford, P. Synthesis and reactions of β-diketiminate-supported complexes with Mg-Fe or Yb-Fe bonds. *Chem. Commun. (Cambridge, U. K.)* **2013**, *49*, 3315−3317.
(81) Blake, M. P.; Kaltsoyannis, N.; Mountford, P. Heterobimetallic complexes containing Ca-Fe or Yb-Fe bonds: Synthesis and molecular and electronic structures of $[MCpFe(CO)_{22}(THF)_3]_2$ (M = Ca or Yb). *J. Am. Chem. Soc.* **2011**, *133*, 15358−15361.
(82) Nippe, M.; Goodman, S. M.; Fry, C. G.; Berry, J. F. Chemically reversible four-electron oxidation and reduction utilizing two inorganic functional groups. *J. Am. Chem. Soc.* **2011**, *133*, 2856−2859.
(83) Brown, J. L.; Fortier, S.; Wu, G.; Kaltsoyannis, N.; Hayton, T. W. Synthesis and spectroscopic and computational characterization of the chalcogenido-substituted analogues of the uranyl ion, $[OUE]^{2+}$ (E = S, Se). *J. Am. Chem. Soc.* **2013**, *135*, 5352−5355.
(84) Pandey, K. K.; Patidar, P. Theoretical investigation of M≡E bonds in transition metal−ylidyne complexes *trans*-$[H(PMe_3)_4M{\equiv}ER]$ (M = Mo, W); E = Si, Ge, Sn, Pb; R = Mes, Xylyl). *J. Organomet. Chem.* **2012**, *702*, 59−66.
(85) Purgel, M.; Maliarik, M.; Glaser, J.; Platas-Iglesias, C.; Persson, I.; Tóth, I. Binuclear Pt-Tl bonded complex with square pyramidal coordination around Pt: A combined multinuclear NMR, EXAFS, UV−Vis, and DFT/TDDFT study in dimethylsulfoxide solution. *Inorg. Chem.* **2011**, *50*, 6163−6173.
(86) Barysz, M.; Pyykkö, P. Strong chemical bonds to gold. High level correlated relativistic results for diatomic $AuBe^+$, AuC^+, $AuMg^+$, and $AuSi^+$. *Chem. Phys. Lett.* **1998**, *285*, 398−403.
(87) Le, A.; Heaven, M. C.; Steimle, T. C. The permanent electric dipole moment of thorium sulfide, ThS. *J. Chem. Phys.* **2014**, *140*, No. 024307.
(88) Gagliardi, L.; Pyykkö, P. Theoretical search for very short metal-actinide bonds: NUIr and isoelectronic systems. *Angew. Chem., Int. Ed.* **2004**, *43*, 1573−1576;German ed.: *Angew. Chem.* **2004**, *116*, 1599−1602.
(89) Santos, M.; Marçalo, J.; Pires de Matos, A.; Gibson, J. K.; Haire, R. G. Actinide-transition metal heteronuclear ions and their oxides $[IrUO]^+$ as an analogue to uranyl. *Eur. J. Inorg. Chem.* **2006**, *2006*, 3346−3349.
(90) Pyykkö, P.; Li, J.; Runeberg, N. Quasirelativistic pseudopotential study of species isoelectronic to uranyl and the equatorial coordination of uranyl. *J. Phys. Chem.* **1994**, *98*, 4809−4813.
(91) Gong, Y.; Wang, X.-F.; Andrews, L.; Schlöder, T.; Riedel, S. Infrared spectroscopic and theoretical investigations of the OUF_2 and $OThF_2$ molecules with triple oxo bond character. *Inorg. Chem.* **2012**, *51*, 6983−6991.
(92) Andrews, L.; Wang, X.-F.; Lindh, R.; Roos, B. O.; Marsden, C. J. Simple $N{\equiv}UF_3$ and $P{\equiv}UF_3$ molecules with triple bonds to uranium. *Angew. Chem., Int. Ed.* **2008**, *47*, 5366−5370.
(93) Vlaisavljevich, B.; Gagliardi, L.; Wang, X.-F.; Liang, B.-Y.; Andrews, L.; Infante, I. U and P_4 reaction products: A quantum chemical and matrix isolation spectroscopic investigation. *Inorg. Chem.* **2010**, *49*, 9230−9235.
(94) Pyykkö, P.; Laakkonen, L. J.; Tatsumi, K. REX calculations. 12. Iteration parameters for the 5f-element organometallics of thorium-neptunium. Geometries of ThO_2 and UO_2^{2+} revisited. *Inorg. Chem.* **1989**, *28*, 1801−1805.
(95) King, D. M.; Tuna, F.; McInnes, E. J. L.; McMaster, J.; Lewis, W.; Blake, A. J.; Liddle, S. T. Isolation and characterization of a uranium(VI)-nitride triple bond. *Nat. Chem.* **2013**, *5*, 482−488.
(96) Krechivska, O.; Morse, M. D. ZrFe, a sextuply-bonded diatomic transition metal? *J. Phys. Chem. A* **2013**, *117*, 992−1000.
(97) Wang, H.; Die, D.; Wang, H.-Y.; Xie, Y.-M.; King, R. B.; Schaefer, H. F., III Molecular orbital interpretation of the metal-metal multiple bonding in coaxial dibenzene dimetal compounds of iron, manganese, and chromium. *Theor. Chem. Acc.* **2014**, *133*, No. 1459.
(98) Vegard, L. Die Konstitution der Mischkristalle und die Raumfüllung der Atome. *Z. Physik* **1921**, *5*, 17−26.
(99) López-Pérez, W.; Simon-Oliveira, N.; Molina-Coronell, J.; González-García, A.; González-Hernández, R. Structural parameters, band-gap bowings and phase diagrams of zinc-blende $Sc_{1-x}In_xP$ ternary alloys: A FP-LAPW study. *J. Alloys Compd.* **2013**, *574*, 124−130.
(100) Beagley, B. Empirical relationships between tetrahedral covalent radii and effective nuclear charge. *Chem. Commun. (Cambridge, U. K.)* **1966**, 388−389.
(101) Gao, G.-Y.; Ashcroft, N. W.; Hoffmann, R. The unusual and the expected in the Si/C phase diagram. *J. Am. Chem. Soc.* **2013**, *135*, 11651−11656.
(102) Brunetta, C. D.; Brant, J. A.; Rosmus, K. A.; Henline, K. M.; Karey, E.; MacNeil, J. H.; Aitken, J. A. The impact of three new quaternary sulfides on the current predictive tools for structure and composition of diamond-like materials. *J. Alloys Compd.* **2013**, *574*, 495−503.
(103) López-Vergara, F.; Galdámez, A.; Manríquez, V.; Barahona, P.; Peña, O. $Cu_2Mn_{1-x}Co_xSnS_4$: Novel kësterite-type solid solutions. *J. Solid State Chem.* **2013**, *198*, 386−391.

(104) Lu, J.-B.; Dai, Y.; Guo, M.; Wei, W.; Ma, Y.-D.; Han, S.-H.; Huang, B.-B. Structure and electronic properties and phase stabilities of the $Cd_{1-x}Zn_xS$ solid solution in the range of $0 \leq x \leq 1$. *ChemPhysChem* **2012**, *13*, 147−154.
(105) Burton, L. A.; Walsh, A. Phase stability of the earth-abundant tin sulfides SnS, SnS_2, and Sn_2S_3. *J. Phys. Chem. C* **2012**, *116*, 24262−24267.
(106) Madouri, D.; Ferhat, M. How do electronic properties of conventional III-V semiconductors hold for the III-V boron bismuth BBi compound? *Phys. Status Solidi B* **2005**, *242*, 2856−2863.
(107) Lü, T.-Y.; Zheng, J.-C. Electronic properties of pseudocubic IV-V compounds with 3:4 stoichiometry: Chemical trends. *Chem. Phys. Lett.* **2010**, *501*, 47−53.
(108) DeKock, R. L.; Strikwerda, J. R.; Wu, E. X. Atomic size, ionization energy, polarizability, asymptotic behavior, and the Slater-Zener model. *Chem. Phys. Lett.* **2012**, *547*, 120−126.
(109) Agmon, N. Covalent radii from ionization energies of isoelectronic series. *Chem. Phys. Lett.* **2014**, *595*−*596*, 214−219.
(110) Bohórquez, H. J.; Boyd, R. J. Is the size of an atom determined by its ionization energy? *Chem. Phys. Lett.* **2009**, *480*, 127−131.
(111) Slater, J. C. Atomic shielding constants. *Phys. Rev.* **1930**, *36*, 57−64.